한국생산제조시스템학회지 Vol.21 No.3 2012. 6. pp. 479~486
Journal of the Korean Society of Manufacturing Technology Engineers

기술논문

Analysis and Design of 3-DOF Parallel Mechanism Based on Kinematic Couplings

Weijun Wang*, Changsoo Han+

(논문접수일 2012. 05. 03, 수정일 2012. 05. 31, 심사완료일 2012. 06. 05)

기구학적 커플링으로 구성된 3자유도 병렬 메커니즘 해석 및 설계

왕위준*, 한창수+

Abstract

This paper presents a high-speed automatic micro-alignment system that is a part of an inspection machine for small-sized molded lenses of mobile phones, palm-top computers, and so on. This work was motivated by the shortcomings of existing highest-grade commercial machine. A simple tip/tilt/Z parallel mechanism is designed based on kinematic couplings, which is a 3-degree-of-freedom (3-DOF) moderate-cost alignment stage. It is used to automatically adjust the posture of each lens on the tray, which is impossible by the conventional instrument. Amplified piezoelectric actuators are used to ensure the accuracy and dynamic response. Forward kinematic analysis and simulation show that the parasitic motion is small enough compared to the actuator stroke. From the workspace analysis of the moving platform, it is clear that the output motion range satisfies the design requirements.

Key Words : Kinematic couplings(기구학적 커플링), Pseudo-rigid-body model(의사강체모델), Amplified piezoelectric actuators(증폭압전구동기), Micro-adjustment mechanism(미세조정 메커니즘), Kinematic analysis(기구학 해석)

1. Introduction

As mobile phone becomes more intelligent, smaller and thinner, one of the most important and indispensable components is its built-in camera. One important criterion which determine the quality of the camera is lens. After manufacturing lens, how to detect defects and how to evaluate various performances are very important working procedure. There are several performance indices such as contrast transfer function (CTF) and modulation transfer function (MTF), which are precise measures in frequency domain to specify resolution and perceived sharpness of the lens.

There are two different measuring techniques and corresponding devices. One device is composed of single- pocketed platform that can be moved up and down either by human operator or by motor. Human operator or an image processing algorithm determines “pass or fail” based on the sequence of images of standard chart while moving up. This device has limitation of flexibility: the imaging sensor is the same sensor in phone camera and, hence, should be changed as target model is changed. The other device consists of lens tray with tens of pockets and an additional 2-DOF XY-stage is used to position

* 한양대학교 대학원 기계공학과
+ 교신저자, 한양대학교 기계공학과 (cshan@hanyang.ac.kr)
주소: 426-791 경기도 안산시 상록구 한양대학로 55

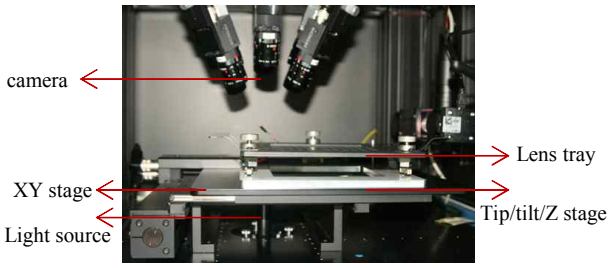

Fig. 1 Prototype of adjustment stage

each pocket to the sensor. The machine, finds the MTF itself rather than images and, hence, it is more flexible. However the machine still has limitations: (1) false fail- detection due to the unexpected or unadjustable inclination of individual lens and (2) slight out-of-focus due to flatness error of the XY stage.

A tray adjustment mechanism need to be augmented to solve these problems. The inclination problem need a tip/tile mechanism and the out-of-focus problem requires a vertical linear mechanism. In order to meet these two alignment requirements, the system needs to have 1-DOF linear motion and 2-DOF tip/tilt motion. The main purpose of the paper is to design a 3-DOF tip/tilt/z parallel mechanism. The prototype of the stage is shown in Fig. 1.

The rest of this paper is organized as follows. Overall structure of 3-DOF tip/tilt/Z mechanism will be presented in section 2, which contains the design configurations, shape parameters and design requirements. The design steps of adjustment stage based on the kinematic couplings are also shown. In section 3, an mathematical model is built via pseudo-rigid-body method and then the forward kinematics and the inverse kinematics are analyzed. Workspace analysis and simulation are explained in Section 4. Finally, concluding remarks are given in Section 5.

2. Design of 3-DOF adjustment mechanism

In the first section, parallel-type mechanism is chosen to achieve the required degree of freedom. The 3-DOF manipulator possesses following characteristics: the link joints with the base are revolute, while the joints on the moving platform are ball-and-socket joints connected to prismatic actuators allowing the variation of the link lengths[1]. This type robot has been developed to different models. A spatial 3-DOF tele-micromanipulator for precise position is a parallel-type mechanism which contains three flexure hinges based serial chains, it was successfully implemented to tele-micromanipulation system[2], however, its disadvantages are small top platform and large size for some applications. A new design of 3-DOF micro-positioning table utilizing three piezoelectric actuators has high stiffness and very little mechanical damping[3]. Its advantage is to utilize three notch flexure hinges for guidance of the moving platform and preload for actuators. Of course, heavy weight, large size and small workspace make it have a small application field. Another using the piezoelectric actuator and amplifier mechanism with flexure hinge as one chain, a 3-DOF parallel type of ultra-precision manipulator for high precision positioning is developed[4]. Its advantage is amplifier mechanism which is designed to extend the motion range because of small motion range of piezoelectric actuator, however, large size and heavy weight make its application limited. Based on the tripod parallel mechanism, an actuation unit utilizing the piezoelectric transducer and flexure hinge, a 3-DOF micro-stage is constructed with such merits as compactness and lightness in its structure[5].

In the paper, a new attempt for 3-DOF adjustment is proposed on the tripod parallel mechanism and kinematic couplings. Firstly, concept for adjustable kinematic coupling is described. And then, one of the chains of parallel mechanism is designed via combining the kinematic coupling with actuator. This chain must satisfy the rule of tripod parallel mechanism, which DOF of one chain is five.

2.1 Kinematic Coupling

When designing a coupling, it is very important to choose the coupling type. The different coupling types is up to the basic types of contact which between the coupled interfaces, such as surface, line and point contact. There are several different coupling types, such as pin joints and elastic averaging coupling, quasi-kinematic coupling and kinematic coupling. Pin joints and elastic averaging coupling are surface contact, its stiffness and load capacity are very high, however, repeatability is poor. In order to obtain the excellent repeatability, kinematic coupling using individual point contacts that each constrain a single degree of freedom is used to adjustment mechanism widely, while load capacity and stiffness are limited by Hertzian contact stress.

Kinematic couplings are couplings that exactly constrain components, and one of a component is constrained by a number of points equal to the number of degrees of freedom.

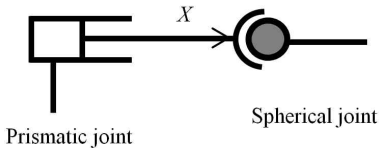

Fig. 2 Pseudo-kinematic model of Ball-Vee groove coupling

The most common combination of kinematic coupling is the ball-groove coupling, which interfaces three balls on one component to three grooves on the opposite component.

A ball on a vee groove is shown in Fig. 3(a). Ball is restricted in the z and y directions, so degree of constraint is two. On the other hand, ball can move along x axis, and rotate about x, y and z axes, therefore, degree of freedom of the ball is four. If we consider the Ball-Vee groove-coupling as a real joint without thinking about the deformation of the ball and vee groove, which means the degree of freedom of this joint is four.

In order to build the statics and dynamics model, we should find other joints to instead of Ball-Vee groove coupling. From the above analysis, we know the Ball-Vee groove coupling is a 4-DOF joint, one direction linear motion and three rotation motions about three axes. Therefore, one direction linear motion can be treated as a prismatic joint, and three rotation motions can be treated as a spherical joint. Pseudo-rigid model of Ball-Vee groove coupling is shown in Fig. 2.

2.2 System configuration

From the theory of tripod parallel mechanism, a tip/tilt/Z adjustment mechanism need three chains at least, and for fully parallel mechanism, the number of chains is strictly equal to the number of DOF of the end-effector. We have already known that a Ball-Vee groove coupling can be considered as a 4-DOF joint, if a 1-DOF joint is used to combine with a Ball-Vee groove coupling to form a new chain, which means the DOF of this new chain is five. In the paper, an amplified pizeoelectric actuator (APA) is used as input joint, which is a 1-DOF prismatic joint. Diagram of the adjustment mechanism is shown as Fig. 3(a). In order to obtain a good stability in a three Ball-Vee groove kinematic coupling, the normal to the planes containing the contact force vector pairs should bisect the angles between the balls[6]. According to Grubler's formula for three dimensional mechanism, the mobility of three-chain adjustment mechanism is

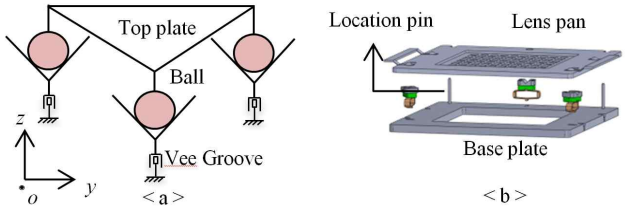

Fig. 3 Schematic diagram of (a) a general adjustment mechanism based on Ball-Vee groove couplings and (b) the proposed configuration

$$m = 6(n-j-1) + \sum_{i=1}^{j} f_i, \tag{1}$$

where n is total number of rigid bodies of mechanism, j is total number of joints and f_i is the number of freedom of joint i. For the mechanism shown as Fig. 3(a), the quantity of n, j and f_i is 5, 6 and (1, 1, 1, 4, 4, 4), respectively. So the mobility of this three-chain adjustment mechanism is 3, which is equal to the number of the actuators. Fig. 3(b) shows the schematic diagram of the proposed adjustment mechanism, which consists of the lens tray to support the detected lens, three actuation units and the base plate to install the actuation units. For this proposed adjustment mechanism, some special designs are described in detail in what follows.

In contrast to the configuration in Fig. 3(a) and 3(b), three balls are fastened on the lens tray with regular measurement, lens tray play a role of top plate to decrease the outside load. The output direction of three actuation units is orthometric with the output of three actuators. Since all actuators are placed horizontally, this can decrease the height of the adjustment stage. And flexible unit play a double roles, one is to change the actuator output direction, and another is to increase the horizontal stiffness and the natural frequencies of the modes related with X and Y translations and Z rotation.

2.3 Design of an adjustment mechanism

In the previous subsection, several basic mechanisms are determined to use for the adjustment system, next according to the design specification to select the model of the actuator, to decide the dimensions of the Ball-Vee coupling and its distribution on the base plate. Before designing this adjustment mechanism, the expected specification of the tip/tilt/Z stage is shown as Table 1. Next, according to the design steps of kinematic coupling and adjustment mechanism, there are three steps to determine the structure of the adjustment stage.

Table 1 Specification of the tip/tilt/z stage

Specification	Unit	Research Target
Lens platform rotation	mrad	0.5
Lens platform motion	μm	100
Outline dimension (W/L/H)	mm	200/200/40~50

Step 1: Design of kinematic couplings

In order to use the kinematic coupling as a part of adjustment, there are several factors to consider, such as the effect of the kinematic couplings stability to whole adjustment, the working life which is affected by the coupling material, coupling stiffness and reaction loads. Six steps stiffness modeling strategies show the details of the modeling the performance and characteristics of kinematic couplings[7]. Friction-based design of kinematic couplings is explained, which concentrates on the ability to reach the centered position of the kinematic couplings[8].

For good stability in a three-groove kinematic coupling, the distribution of three grooves in the base plate is an important design parameter. With an example of a planar kinematic coupling, geometry distribution and direction of three grooves determine the coupling centroid[6], which is an intersection point of angle bisector of the coupling triangle. In the paper, the coupling centroid and triangle's centroid are coincided at the same point, which a coupling where the balls lay on the vertices of an equilateral triangle can make the angle bisectors intersect at the triangle's centroid.

It is important to think about the friction affects for the design of kinematic couplings. One aspect is the choice of material for the ball and grooves. Several techniques can be used to minimize the effect of friction, including low coefficient of friction materials such as Titanium Nitride, Silicon Nitride, harden steel. Moreover, several surface treatment methods also can minimize the effect of friction, such as surface finish, debris removing, and fretting corrosion. Another aspect is the angle of each surface from plane to vees. Since the limiting coefficient of friction is different as the change of angle for the three-vee couplings. The three-vee coupling has slightly better centering ability at the nearly optimal angle[8]. In the paper, material of three-vee groove and ball is harden steel, and under the cover of three-vee groove, a thin Titanium Nitride plate is pasted to minimize the effect of friction.

Step 2: Arrangement of actuator for the kinematic couplings-based adjustment

In order to achieve the function of positioning and fixture based on the kinematic couplings, the concept of hybrid positioner-fixture is developed[9], which designed a six-axis adjustable coupling, moving groove and eccentric ball. According to degree of freedom of motion platform, the adjustable coupling should be designed to have a relative independent position inputs.

In the paper, a 3-DOF tip/tilt/Z motion should be produced for the top component, and in the former description, the lens tray is chosen to instead of the top component, at the same time, the three balls are fixed at the lens tray. In order to avoid changing the structure of the lens tray, three grooves are driven by three actuators to produce motion in the vertical direction, respectively. The S series amplified pizeoelectric actuator - APA120s is selected to produce displacement about 140μm, which produce horizontal motion via piezoelectric actuator, but flexure mechanical element change the horizontal motion to vertical motion. Its performances are shown in detail[10].

Step 3: Combine the actuating device with the kinematic coupling

After the step 1 and step 2, the style of kinematic coupling, the distribution of three grooves in the base plate and driven approach are determined completely. Next step is to design the three driven elements.

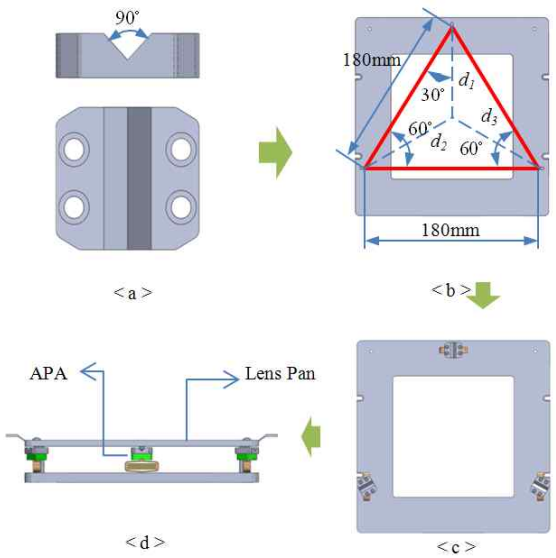

Fig. 4 The adjustment stage design steps, (a) design the kinematic couplings, (b) arrange the actuator for the kinematic couplings-based adjustment, (c) combine the actuating device with the kinematic coupling to fix at the baseplate and (d) the whole adjustment stage based on the kinematic coupling and flexure actuator

Fig. 4 describes the design steps of kinematic coupling-based adjustment stage, and give several design parameters which is according to the system demands. After the adjustment stage is designed, its kinetic characteristic should be check whether its output can satisfy the design goals or not.

3. Pseudo-rigid model and analysis

In the second section, the APA and ball-vee coupling are modeled as a conventional 1-DOF prismatic, 1-DOF prismatic, and 3-DOF spherical joints, the system is kinematically determine and the mobility of the system is 3. Fig. 5 shows a 3-PPS schematic diagram of the system, where symbols are also introduced. In each lamb, the prismatic joint attached to the base is vertical and actuated, while the other prismatic joint is horizontal and passive. And the three lambs remain in three vertical planes, called the restricting planes, which intersect to a common line at an angle of 120°, and the centers of the spherical joints form an equilateral triangle.

Below is the explanation of the symbols:

$\hat{e_i}$ Unit vector for the direction of the foot of the limbs (i = 1, 2, 3)

$\hat{e_z}$ Unit vector of the vertical direction

a_i Distance from the origin to every lamb

q_i The distance from Ai to Bi via actuator output

x_i The distance from B_i to C_i via spherical joint changing

The location of the spherical joint C_i relative to the origin can be described as

$$s_i = (a_i + x_i)\hat{e_i} + q_i\hat{e_z} \tag{2}$$

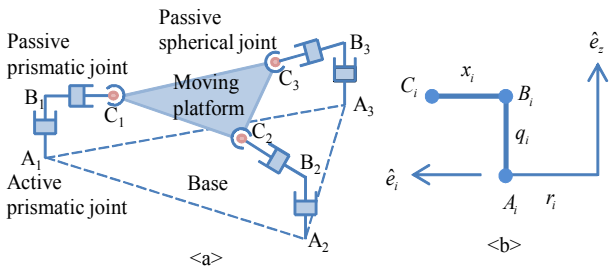

Fig. 5 Schematic diagram of (a) 3-PPS parallel adjustment and (b) details of symbol explanation

There are several literatures on the 3-PPS parallel mechanism, studying its kinematics, singularity analysis and design[11,12]. In the paper, forward and inverse kinematics is studied to explain the precision of the kinematic coupling adjustment. And workspace of 3-PPS is taken into account.

3.1 Forward kinematics

The purpose of the forward kinematics is to calculate the configuration (position p and rotation R) of the moving platform via given passive joint output. From the constraints imposed on the chain, the position of the prismatic joint can be determined, and then the position of spherical joint can be calculated along the chain. Next, the position and orientation of the moving platform will be described from the three parts.

Firstly, position of spherical joints is obtained from the active joints variable. From the fact that the mutual distance c_{ij} between spherical joints C_i and C_j should be constant, the mutual distance can be calculated as

$$s_i - s_j = (a_i + x_i)\hat{e_i} + q_i\hat{e_z} - (a_j + x_j)\hat{e_j} - q_j\hat{e_z} \tag{3}$$

We can make the squaring operation for both sides of Eq. (3) to obtain

$$\begin{aligned} s_{ij}^2 = {} & (a_i + x_i)^2 + (a_j + x_j)^2 + (q_i - q_j)^2 \\ & - 2(a_i + x_i)(a_j + x_j)\rho_{ij} \end{aligned} \tag{4}$$

where $\rho_{ij} = \hat{e_i} \cdot \hat{e_j}$, $\hat{e_i} \cdot \hat{e_i} = 1$ and $\hat{e_i} \cdot \hat{e_z} = 0$. Substituting i with 1, 2, and 3 into Eq. (4), we get the equations as

$$\begin{aligned} f_1 = {} & (a_2 + x_2)^2 + (a_3 + x_3)^2 \\ & - 2(a_2 + x_2)(a_3 + x_3)\rho_{23} - b_{23} = 0 \\ f_2 = {} & (a_3 + x_3)^2 + (a_1 + x_1)^2 \\ & - 2(a_3 + x_3)(a_1 + x_1)\rho_{31} - b_{31} = 0 \\ f_3 = {} & (a_1 + x_1)^2 + (a_2 + x_2)^2 \\ & - 2(a_1 + x_1)(a_2 + x_2)\rho_{12} - b_{12} = 0 \end{aligned} \tag{5}$$

where $b_{ij} = s_{ij}^2 - (q_i - q_j)^2$. Eq. (5) is a nonlinear equation and it is difficult to find the exact solution. By using Newton's method to obtain the approximated equation, it is efficient to solve this nonlinear equation. Furthermore, the output of APA is so small that it will not affect the results effectively.

Eq. (5) can be described into vector equation as

$$f(x) = 0 \tag{6}$$

where $x=(x_1,x_2,x_3)$, and by using Newton's method, approximated equation which is derived from Eq. (6) is shown as

$$x^0=0 \qquad (7)$$
$$x^k=x^{k-1}-(\frac{\partial f}{\partial x})^{-1}(x_{k-1})f(x_{k-1})$$

where x^k is the value of x at the k-th iteration. Take the derivative of the Eq. (7) on the both sides, differential equation can be obtained as

$$\frac{\partial f_i}{\partial x_j}=\begin{cases}2(x_j+a_j)-2\rho_{j,j+1}(x_{j+1}+a_{j+1}) & \text{if } i\neq j\\ 0 & \text{if } i=j\end{cases} \qquad (8)$$

Fig. 6 shows the error $\sqrt{\| f \|}$ at first and second step where $x_2,x_3 \subseteq [0,0.2]$ mm while $x_1=0$. It is indicated that the linearized calculation is so accurate that the error in the position of the spherical joint is less than 4×10^{-5} nm, which can be ignored comparing with the actuator stroke.

Secondly, rigid body transfer matrix is determined from the spherical joints position. From the first step, the position vector of the spherical joints has already obtained, so posture of moving platform can be decided. Original coordinate of moving platform can be described from affine combination as follow

$$p=\alpha_1 s_1+\alpha_2 s_2+\alpha_3 s_3, \alpha_1+\alpha_2+\alpha_3=1 \qquad (9)$$

Substitute $s_i=a_i\hat{e_i}$ into the Eq. (9), and express as matrix form like

$$\left[a_1\hat{e_1}\, a_2\hat{e_2}\, a_3\hat{e_3}\right]\alpha=A\alpha=0 \qquad (10)$$

So α can be calculated from the null space of the matrix A. Now the position of the origin has already obtained, in order to get the posture of moving platform, the rotation matrix should be derived as follow.

The relationship of position of the spherical joints and rigid body transfer matrix is shown as Fig. 7. Rotation matrix is

$$R=[r_1\, r_2\, r_3] \qquad (11)$$

From the Fig. 7, vector r_3 can be described by three spherical joint positions, which is the plane normal vector.

$$r_3=(s_2-s_1)\times(s_3-s_1) \qquad (12)$$
$$=b_1\times b_2+b_2\times b_3+b_3\times b_1$$

and the first row vector r_1 of Eq. (11) is

$$r_1=\frac{s_1-p}{a_1} \qquad (13)$$

and the second row vector r_2 of Eq. (11) is

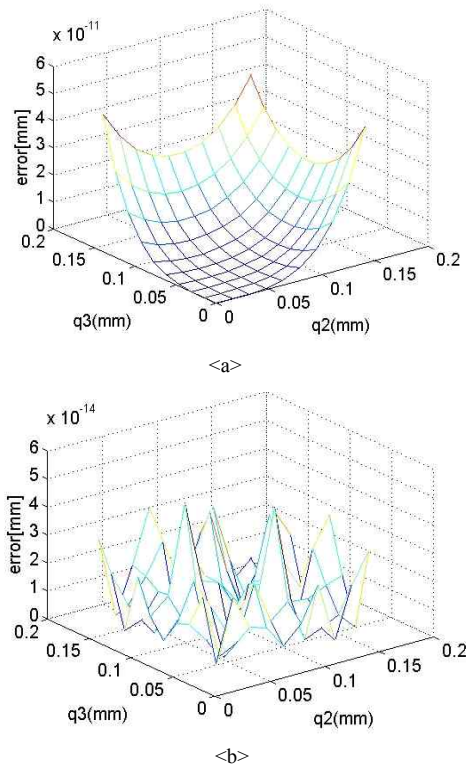

Fig. 6 Effectiveness of linearized forward kinematics of 3-mobility model, (a) single iteration and (b) two iterations simulation

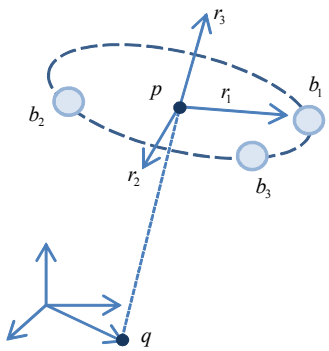

Fig. 7 Relationship of spherical joints position and rigid body transfer matrix

$$r_3 = r_1 \times r_2 \tag{14}$$

By using Eqs. (10) - (14), the rigid body transfer matrix can be derived completely.

Finally, the tip/tilt angle can be determined from the rotation transfer matrix if the input values are given. Make the detail of Eqs. (11) as follow matrix.

$$R = \begin{bmatrix} r_{11} r_{12} r_{13} \\ r_{21} r_{22} r_{23} \\ r_{31} r_{32} r_{33} \end{bmatrix} \tag{15}$$

Tip/tilt of the adjustment stage can be described as ϕ_x, ϕ_y at the local coordinate system. And there is another method to describe the orientation of the moving platform, which is equivalent angle-axis representation. Next two equations will be used to calculate the vector ω and angle θ according to the given rotation matrix *R*.

$$\theta = \arccos \frac{tr(R) - 1}{2} \tag{16}$$

$$\omega = \frac{1}{2\sin\theta} \begin{bmatrix} r_{32} - r_{23} \\ r_{13} - r_{31} \\ r_{21} - r_{12} \end{bmatrix} \tag{17}$$

So tip/tilt of the moving platform can be calculated as

$$\phi_x = \theta\omega_1, \phi_y = \theta\omega_2 \tag{18}$$

3.2 Inverse kinematics

The inverse kinematics is somewhat simple if the configuration of the moving platform is given. If the tip/tilt ϕ_x, ϕ_y of the platform is given, and rotation transfer matrix is expressed as follow

$$R = \begin{bmatrix} 1 & 0 & 0 \\ 0 & c_x & -s_x \\ 0 & s_x & c_x \end{bmatrix} \begin{bmatrix} c_y & 0 & s_y \\ 0 & 1 & 0 \\ -s_y & 0 & c_y \end{bmatrix} = \begin{bmatrix} c_y & 0 & s_y \\ s_x s_y & c_x & -s_x s_y \\ -c_x s_y & s_x & c_x c_y \end{bmatrix} \tag{19}$$

where $s_x = \sin\phi_x$, $c_x = \cos\phi_x$, and so on.

If the position of the platform p_z is given, moving vector *p* can be calculated as

$$p = [0\ 0\ p_z]^T \tag{20}$$

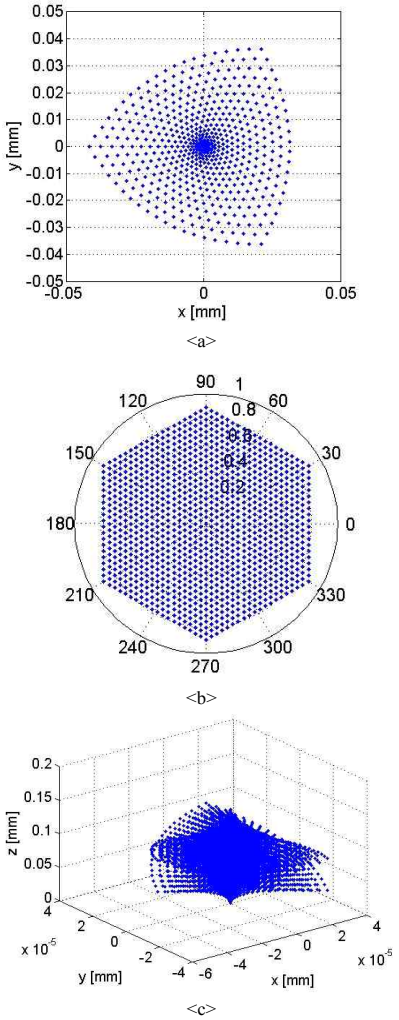

Fig. 8 Workspace of 3-PPS parallel adjustment stage, (a) xy-position, (b) xy-orientation of polar plot and (c) z-position

If the rotation and position *(R, p)* of moving platform are determined, the position of spherical joints can be calculated by

$$s_i = a_i R\hat{e}_i + p, (i = 1,2,3) \tag{21}$$

And then the active moving joints q_i and passive moving joints x_i can be calculated by

$$\begin{aligned} q_i &= s_i \cdot \hat{e}_z \\ x_i &= s_i \cdot \hat{e}_i \end{aligned} \tag{22}$$

4. Workspace analysis

The workspace can be visualized by plotting the image of the sufficiently dense grid of the joint space, which is explained as

$$\{(q_1,q_2,q_3) : q_1,q_2,q_3 = k\triangle q,\ k = 0,1,\cdots,N\} \quad (23)$$

Fig. 8 shows the result with $\triangle q = 0.02$ and $N = 20$. The sensitive motions of the system are *z*-translation and *xy*-rotation. Since the *z*-translational motion is quite straightforward, the *xy* parasitic motion is plotted instead. The rotational displacement is decomposed into *xy*- and *z*-components and *xy* component is plotted in polar form.

5. Conclusions

The main contribution of this paper is to design a 3-DOF adjustment stage for lens inspection, which is based on the kinematic coupling and flexure input actuators. In order to adjust the pose of lens tray precisely, flexure-based amplified piezoelectric actuator is used to give the input to the whole system, which can make the motion smooth. Also, in order to decrease the weight of the load and support a large moving plate, kinematic coupling is used. It is worth mentioning that kinematic coupling-based adjustment stage can be integrated into the characteristics of the lens tray, which utilize the lens tray in the place of moving plate.

Forward kinematic analysis and simulation results showed that the parasitic error is less than 0.04 mm, which is small enough compared with the actuator's stroke 0.2 mm. From the workspace analysis of the moving platform, it is clear that the output motion range is 0.6 mrad for tip/tilt and 0.2 mm for z-motion, which satisfies the design requirements in Table 1.

Acknowledgement

This research was supported by the MKE (The Ministry of Knowledge Economy), Korea, under the 'Advanced Robot Manipulation Research Center' support program supervised by the NIPA (National IT Industry Promotion Agency) (NIPA-2012-H1502-12-1002)

References

(1) Hunt K. H., 1983, "Structural Kinematics of in Karallel Actuated Robot Arms," T*ransmissions and Automation in design, J. of Mechanisms*, Vol. 105, No. 4, pp. 705~712.

(2) Chung, G. B., Yi, B. J., Suh, I. H., Kim, W. K., and Chung, W. K., 2001, "Design and Analysis of a Spatial 3-DOF Micromanipulator for Tele-operation," *Proc. of IEEE/RSJ Int. Conf. Intell. Robots Syst*., Vol. 1, pp. 337~342.

(3) Zhang D., Chetwynd D. G., Liu X., and Tian Y., 2006, "Investigation of a 3-DOF Micro-positioning Table for Surface Grinding," *Int. J. Mech. Sci.,* Vol. 48, No. 12, pp. 1401~1408.

(4) Lee, J. I., Lee, D. C., and Han, C. S., 2008, "3-DOF Parallel Micromanipulator: Design Consideration," *Transactions of the Korean Society of Machine Tool Engineers*, Vol. 17, No. 2, pp. 13~22.

(5) Kim, H. S., and Cho, Y. M., 2009, "Design and Modeling of a Novel 3-DOF Precision Micro-stage," *Mechatronics*, Vol. 19, No. 5, pp. 598~608.

(6) Slocum, A. H, 1992, *Precision Machine Design, Society of Manufacturing Engineer*, Prentice-Hall, New Jersey, pp. 401~412.

(7) Culpepper, M. L., 2004, "Design of Quasi-kinematic Couplings," *Precision Engineering*, Vol. 28, No. 3, pp. 338~357.

(8) Hale, L. C., 1998, "Friction-based Design of Kinematic Couplings," *Proceedings of ASPE*, pp. 45~48.

(9) Culpepper, M., Kartik, M. V., and DiBiasio, C., 2005, "Design of Integrated Eccentric Mechanisms and Exact Constraint Fixtures for Micron-level Repeatability and Accuracy," *Precision Engineering*, Vol. 29, No. 1, pp 65~80.

(10) Cedrat Technologies, n.d., viewed 8 September 2010, <http://www.cedrat-technologies.com/en/mechatronic-products/actuators/apa.html>

(11) Liu, X. J., Puruschek, P., and Pritschow, G., 2004, "A new 3-DoF Parallel Mechanism with Full Symmetrical Structure and Parasitic Motions," *Proceeding of IMG*, pp. 389~394.

(12) Briot, S., and Bonev, I. A., 2008, "Singularity Analysis of Zero-torsion Parallel Mechanisms," *IEEE International Conference on Intelligent Robots and Systems (IROS)*, pp. 22~26.